THE ASTROPHYSICAL JOURNAL, 218:L121–L127, 1977 December 15

VELOCITY CURVES FOR BROAD AND SHARP COMPONENTS OBSERVED IN THE EMISSION LINES FROM AM HERCULIS

J. L. GREENSTEIN, W. L. W. SARGENT, AND T. A. BOROSON
Hale Observatories, California Institute of Technology, Carnegie Institution of Washington

AND

A. BOKSENBERG*
Department of Physics and Astronomy, University College London
Received 1977 August 29; accepted 1977 October 4

ABSTRACT

We have obtained high-resolution observations of the profiles of the emission lines He I λ4471 and He II λ4686 around a complete cycle of the X-ray binary AM Her. The profiles are resolved into broad (B) and sharp (S) components: velocity curves are given for each component for both the He I and He II lines. The velocity amplitude of the B component is about 4 times that of the S component. The two components vary out of phase by 133° ± 5°. The S component is at conjunction during the soft X-ray eclipse. Implications of these results for models of AM Her are discussed.

Subject headings: stars: variables — X-rays: binaries

I. INTRODUCTION

The magnetic compact variable AM Her is an X-ray source in a complex binary system (Priedhorsky 1977; Cowley and Crampton 1977; Olson 1977; Szkody and Brownlee 1977; Hearn and Richardson 1977). The spectrum shows strong emission lines presumably from gas streams. Coudé spectra with the reticon array taken by Shectman in 1976 (Greenstein, Arp, and Shectman 1977) suggested complex, variable emission structure. Spectrophotometry by Greenstein shows a continuum different from that of AN UMa, another magnetic compact variable (Krzeminski and Serkowski 1977), with a Balmer emission discontinuity and flux decreasing with frequency. The contribution of cyclotron light which produces the linear polarization (Tapia 1977) is largest in the red. Models suggested have a hot spot (Stockman *et al.* 1977; Fabian *et al.* 1977) near a compact, synchronous oblique-rotator with a dipole field $\approx 2 \times 10^8$ gauss; the secondary (not seen) is supposed to be heated by the X-rays. We present observations of the profiles of the He I λ4471 and He II λ4686 emission lines obtained around a complete 3 hour cycle, at higher spectral resolution than any published previously. They show that the He I and He II lines have broad and sharp components which are almost in antiphase. We give velocity curves for these components separately.

II. OBSERVATIONS

The image photon-counting system (IPCS) of University College London was used to observe AM Her on three nights at the Hale telescope coudé spectrograph in 1977 April. Table 1 gives a journal of the observations. The device, which gives simultaneous sky subtraction in 1000 channels, was used in the manner described by Boksenberg and Sargent (1975). The 1″ wide slit subtended two channels, giving an effective resolution of 0.6 Å over a wavelength range of 330 Å. A wavelength scale was established by exposing an Ar-Fe hollow cathode arc before and after each sequence of observations. The seeing disk was variable and always larger than the slit width. Most observations were made of the wavelength region including λλ4471, 4686 emission lines. One observation, detailed in Table 1, was made of the Hα region.

Observations were made in sequences of exposures each lasting 1100 s with 100 s gaps. One sequence, obtained on 1977 April 12–13, consists of nine consecutive exposures and covers almost one cycle (period 11139 s)

TABLE 1

JOURNAL OF OBSERVATIONS OF AM HERCULIS

Record No.	Hel. JD 24 43000+	ϕ_M	1977 April
23.....	239.9782	1746.841	5–6
24.....	239.9921	1746.949	5–6
25.....	240.0060	1747.056	5–6
26.....	240.0198	1747.163	5–6
113.....	245.9581	1793.223	11–12
114.....	245.9721	1793.332	11–12
115.....	245.9859	1793.439	11–12
116.....	245.9998	1793.547	11–12
117.....	246.0137	1793.654	11–12
119*.....	246.0279	1793.765	11–12
141.....	246.8968	1800.504	12–13
142.....	246.9107	1800.612	12–13
143.....	246.9246	1800.720	12–13
144.....	246.9384	1800.827	12–13
145.....	246.9523	1800.935	12–13
146.....	246.9662	1801.042	12–13
147.....	246.9801	1801.150	12–13
148.....	246.9940	1801.258	12–13
149.....	247.0079	1801.366	12–13

* Hα region.

* Guest Investigator, Hale Observatories, 1977.

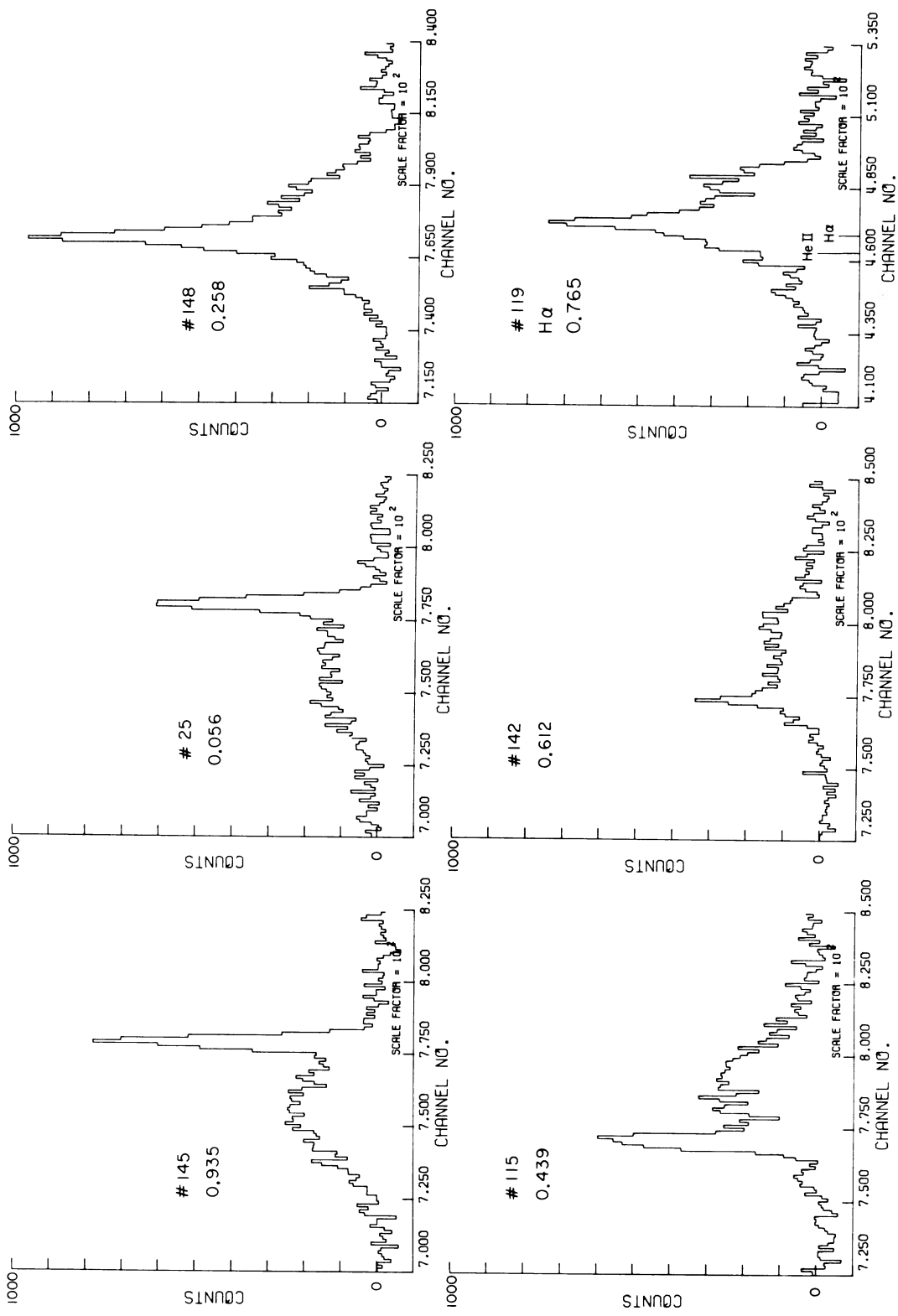

FIG. 1.—Selected observations of photon counts in He II and Hα with continuum subtracted, channel number horizontally, 1100 s integration. Resolution used 0.6 Å (0.9 Å at Hα). The sharp component, which is nearly stationary, is recognizable in only a few channels. The Hα line is blended with He II. Run number and magnetic phase are given.

of the binary orbit. The phases quoted in Table 1 are computed from Tapia's (1977) ephemeris, in which zero phase corresponds to maximum linear polarization.

III. RESULTS

It was found that both the He I λ4471 and He II λ4686 emission lines in Am Her have complex, variable profiles. These can be described in terms of a broad (B) component which exhibits a large periodic excursion in velocity together with a sharp (S) component which exhibits a much smaller periodic variation in velocity. The S and B components, which are clearly resolved for the first time in these observations, vary in velocity 133° out of phase.

Examples of individual profiles are shown in Figure 1, in which there are five observations of the He II λ4686 line at different phases, and one observation of Hα. The velocity scale is 19 km s^{-1} per channel for λ4686 and 21 km s^{-1} per channel at Hα. The relative emission in the two components is seen to fluctuate over the cycle. The FWHM for the S components is 87 km s^{-1}, after correction for instrumental resolution. In order to display the line profile changes more clearly, we show in Figures 2 and 3 isophotal contours for the He II λ4686 line and the He I λ4471 line, respectively. These were generated by computer from the nine IPCS measurements made on one night. No correction was made for gross light variation or for variable transmission through the spectrograph slit. The large phase difference be-

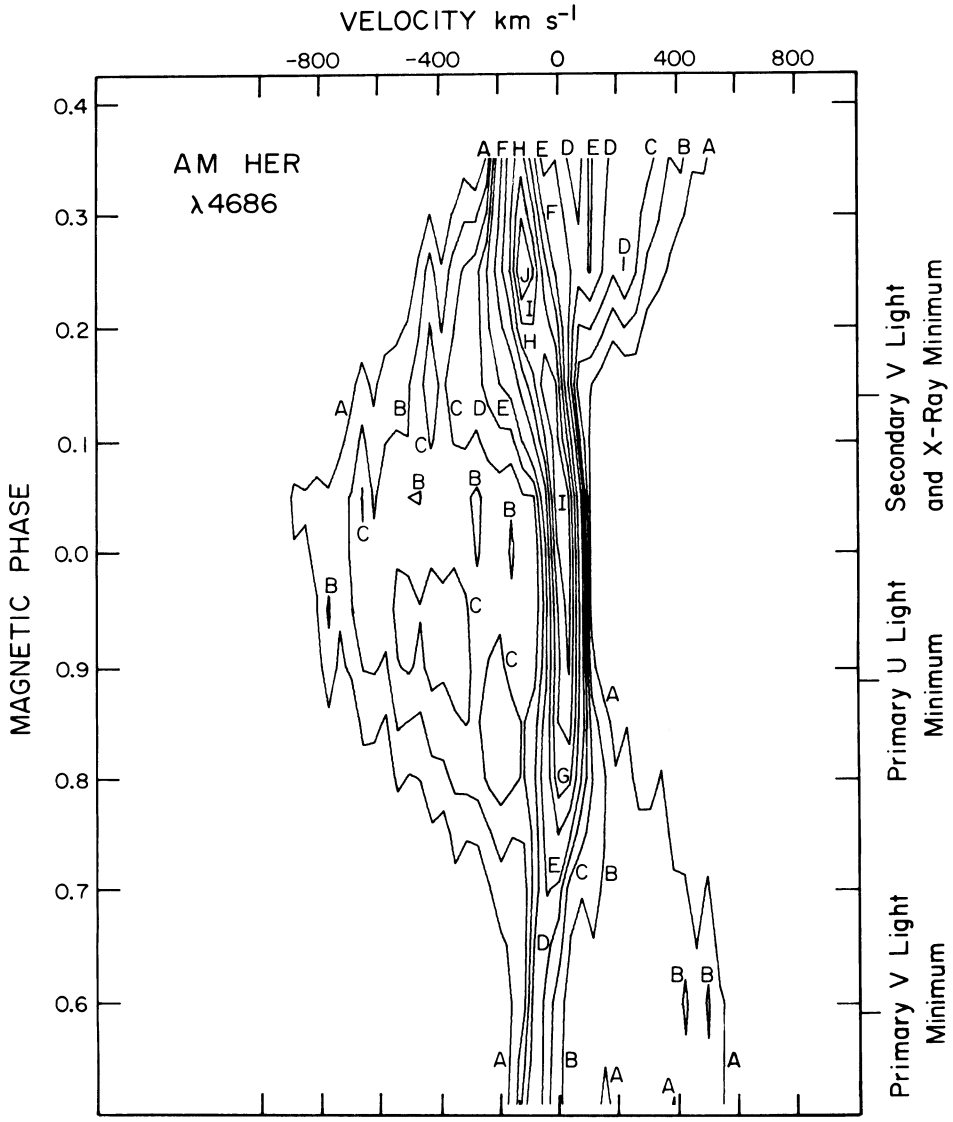

FIG. 2.—The isophotal contours in He II λ4686 are computer-generated from data provided by the nine IPCS runs on one night. No correction is made for gross light variation or transmission through the slit. The sharp and broad S waves are in nearly opposite phase. Events in the light and X-ray fluxes on the right-hand vertical scale. Isophotes are for *A* to *D*, 200 to 500 counts in two channels, and *E* to *J*, 600 to 1600 counts; the velocity scale needs +10 km s^{-1} correction to heliocentric. Time increases vertically.

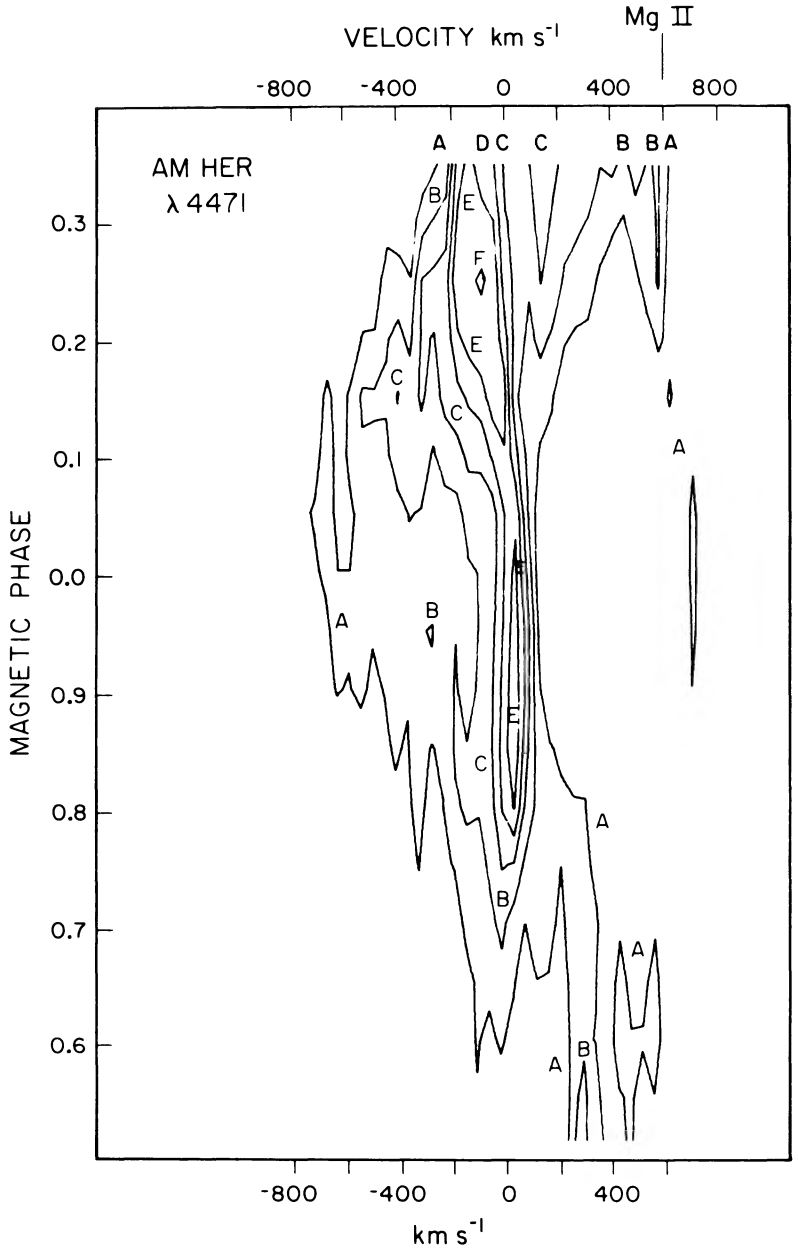

FIG. 3.—Isophotal contours for He I λ4471, *A–E*, 200–600, *F* 800 counts. The two S waves are visible, and details in the sharp component, e.g., a maximum strength near $\phi_M = 0.3$, resemble those in Fig. 2.

tween the B and S components is particularly evident in these figures.

The contour maps and the individual profiles were used in conjunction in order to obtain velocity curves for the B and S emission components in both the He I and He II lines. The position of the central channel was used to give V_S to an accuracy of about ± 10 km s^{-1}. The broad component is approximately symmetrical even when blended at its worst with the sharp component. The midpoint of the broad component could be estimated to give V_B to about ± 50 km s^{-1}. The resulting velocity curves for the B and S components of He II λ4686 are shown in Figure 4. Data points obtained on different nights are shown by different symbols. A sinusoidal (i.e. zero eccentricity) velocity curve was fitted to the 18 data points obtained in three nights to give, for the B and S components,

$$V_B = -22 + 309 \sin 2\pi(\phi_M - 0.283)$$
$$\pm 19 \pm 25 \qquad \pm 0.013 \qquad (1a)$$

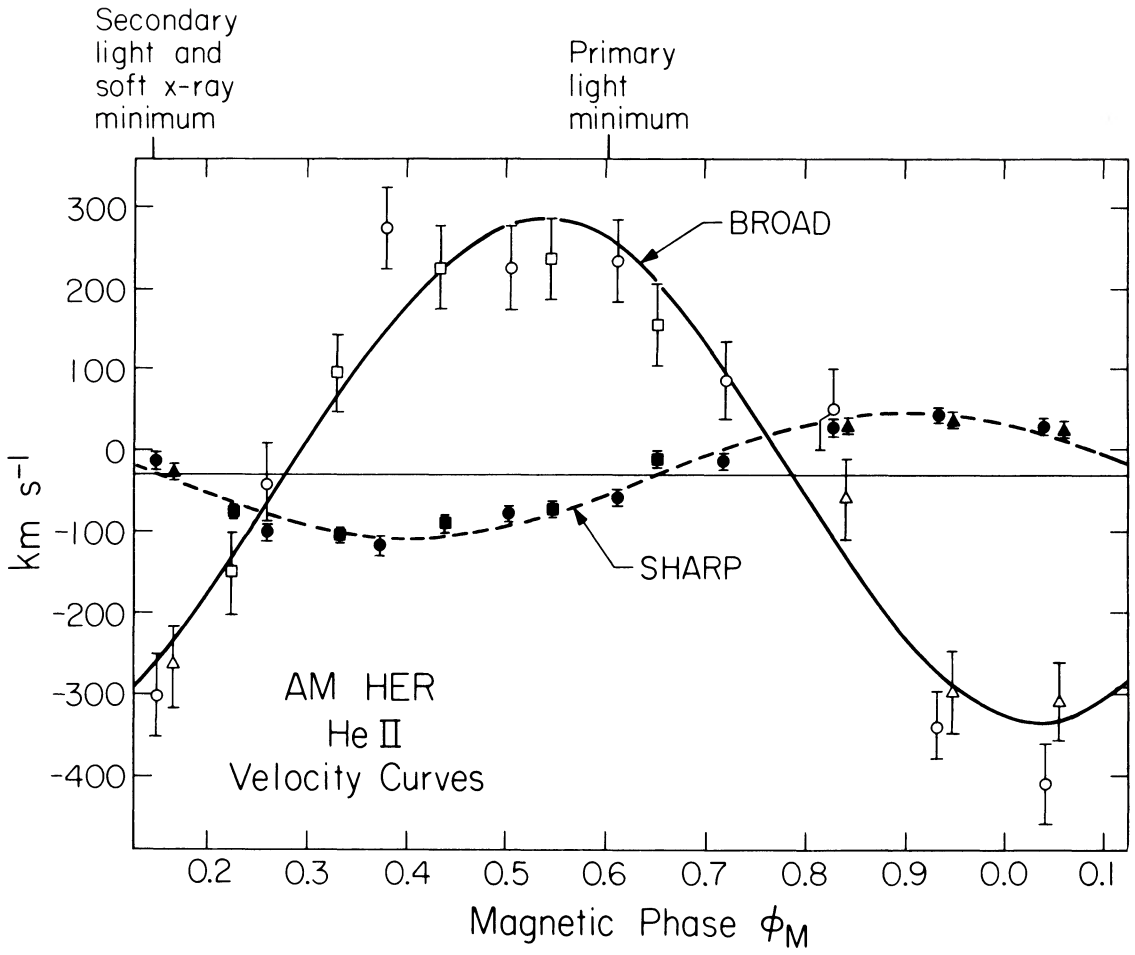

FIG. 4.—Sinusoidal velocity curves (eqs. [1a], [1b]) for the broad and sharp components of He II λ4686 are plotted as function of phase from maximum linear polarization, ϕ_M. The observations are records 23–26, *triangles;* 113–117, *squares;* 141–149, *circles. Open symbols*, the broad component, V_B; *filled symbols*, the sharp component, V_S. The ratio of semiamplitudes $K_B/K_S = 4.08$; the γ-velocities are equal within their error. The top shows events in the light curve and soft X-ray flux.

$$V_S = -30 + 76 \sin 2\pi(\phi_M - 0.653)$$
$$\pm 3 \pm 5 \qquad \pm 0.009. \qquad (1b)$$

The phase difference between the B and S components is 0.370 ± 0.016 or $133 \pm 5°$. The intensity-weighted mean is dominated by light from the B component. Thus, our equation (1a) should and does agree roughly with the values obtained by Priedhorsky (1977) and by Cowley and Crampton (1977). Priedhorsky gives $K_B = 330 \pm 37$ km s^{-1} and $\phi_M°(B) = 0.259 \pm 0.016$. Cowley and Crampton measure a "base" and a "peak" velocity for the blended λ4686 profile; the velocity curve for their "base" follows equation (1a) approximately. Measurement of He I λ4471 proved to be more difficult, since the line is weaker than λ4686 and the sharp component less obvious. The number of measurable velocities is 13 for V_S and 14 for V_B. The derived sine curves were

$$V_B = -8 + 305 \sin 2\pi(\phi_M - 0.280)$$
$$\pm 9 \pm 13 \qquad \pm 0.007, \qquad (2a)$$

$$V_S = -45 + 116 \sin 2\pi(\phi_M - 0.702)$$
$$\pm 8 \pm 11 \qquad \pm 0.013. \qquad (2b)$$

The velocity curves for the B component are identical within the errors of measurement in He I and He II. The mean γ-velocity for the B and S components in both He I and He II lines is -26 ± 15 km s^{-1}, weighting all observations equally. The difference between the four individual γ-velocities is not significant, nor is the difference between the velocity amplitudes of the S component in He I and He II. The phase of V_S differs by 0.049 or 3 σ between He I and He II; the effect is in the sense that He I is more nearly 180° out of phase with V_B than He II. Inspection of individual velocities in Figure 4 shows that V_B may have a somewhat flatter maximum than the sine curve, a distortion sometimes associated with streams in binaries.

The lower contours of λ4686 remain symmetric; at 120 counts the extremes are at −1000 and +700 km s^{-1}. They overlap He I λ4713 at positive and C III lines

(RMT 5) at negative shifts. If the He II atoms were in an intense magnetic field, the quadratic Zeeman effect would produce a broad, violet-shifted extension, for which we have no evidence.

The data from the two other nights generate short segments of isophotes agreeing with Figure 2. Counts on runs 113–117 are higher, and define the behavior of the S ridge when $0.35 < \phi_M < 0.75$. The S gas cannot be totally eclipsed, and varies $\pm 50\%$ in strength. The B gas has a remarkably stable profile, in both height and width, resembling that observed in 1976 (Greenstein, Arp, and Shectman 1977).

IV. MODELS

At $\phi_M = 0$, the linear polarization maximum, the B cloud is at 102° to the line of sight. If cyclotron radiation produces the linearly polarized continuum, magnetic lines of force point toward B, which is at maximum velocity of approach at $\phi_M = 0$.

The integrated flux from a line in the V_S region is about 0.2 that in the V_B region, and the gases producing both are, at most, partially eclipsed. We find that the line intensities (Balmer and He I decrement) and the Balmer emission jump are those of a collisionally excited gas which may have appreciable optical thickness, agreeing with Stockman *et al.* (1977). Such gas clouds can cause line flux variations as their aspect changes. We estimate $n_e^2 V \approx 10^{55}$ to 10^{56} cm^{-3} in the B region if AM Her is at a distance of 100 pc. An upper limit $n_e < 3 \times 10^{14}$ cm^{-3} is set by the Inglis-Teller formula for the Stark effect and the appearance of high quantum number hydrogen lines. An approximate limit comes from the probable minimum value of V if the B gas is near the white dwarf. The magnetic field would produce emission-line shifts; these are absent, since the wavelengths and γ-velocities found here, by Cowley and Crampton (1977), Crampton and Cowley (1977), and Priedhorsky (1977) seem reasonable. From Tapia (1977) Stockman *et al.* (1977), and Michalsky, Stokes, and Stokes (1977), the field is 1 to 2×10^8 gauss. From Kemic (1974), the $2\ ^3P^o$–$4\ ^3D$ line of He I is spread from λ4463 to λ4482 at 10^6 gauss. The larger Coulomb force gives λ4686 He II a smaller quadratic Zeeman effect; from Surmelian and O'Connell (1974*a*, *b*), we estimate $B < 3 \times 10^6$ gauss. Thus the emission lines must be produced outside five white-dwarf radii ($r_Z > 3 \times 10^9$ cm) or $V > 10^{29}$ cm^3, i.e., $n_e \lesssim 10^{13}$ cm^{-3}. The gas cloud resembles a solar prominence in density and in control of its motion by a magnetic field. Let the white dwarf, radius R, have a dipole field $B(r) = B(0)(R/r)^3$. Equating the gravitational potential and the magnetic energies, the Alfvén radius, $r_A \leq 1.54 \times 10^{13}\, n_e^{-1/5}$ cm. We have neglected both rotation and the other star; we find r_A such that the gas corotates with the magnetic field even near the center of mass. If the magnetic field is not synchronous with the orbit but spins rapidly (Fabian *et al.* 1977), a disk could surround the white dwarf. The rotation period at the edge of a disk could be shorter than our integration time, averaging the profile.

Suppose that the B component arises from a gas cloud moving with star B, which we assume to be the white dwarf, and that the S component is associated with star S. Then the mass function $f(m) = 1.035 \times 10^{-7} K_B P_{days} = 0.394\ m_\odot$. The unknown ratio m_B/m_S is limited by the maximum mass for a white dwarf and the fact that the true $K_S > K_S$(obs), i.e., that $m_B/m_S = K_S/K_B > 0.25$. The range of solutions, adopting $\sin^3 i = 1$, is: for $K_S = K_S$(obs), $m_S = 0.61$, $m_B = 0.15_\odot$; for $K_S = 2\,K_S$(obs), $m_S = 0.88$, $m_B = 0.43_\odot$; for $K_S = 3\,K_S$(obs), $m_S = 1.19$, $m_B = 0.88_\odot$. The observed K_S gives an unpleasantly low-mass white dwarf, while the highest K_S gives somewhat too luminous a normal star (late F type) for the system to resemble other U Geminorum stars.

Alternatively, we may assume that the B gas is associated with the normal star and the S gas is located near the white dwarf. The X-ray eclipse is then more simply explained as occultation by the large star or its gas streams. For $K_S = K_S$(obs), the mass m_S is that of a normal degenerate star, and the companion is a late dM. For $K_S = 2\,K_S$(obs) we have a massive white dwarf and an early dM; $K_S = 3\,K_S$(obs) is impossible. However, on this assumption, the question arises of the interpretation of K_B. The B gas cloud would have to envelop the normal star, since it is always visible; its symmetry and velocity spread could not be understood if it were only a hot spot facing the X-ray source.

One difficulty obviously exists if we attempt to describe our observed symmetrical, variable-velocity contours as a result of the varying projection on the line of sight of an accelerating stream (e.g., Michalsky, Stokes, and Stokes 1977). This is easily seen if we adopt solid-body rotation of gas locked onto and flowing along a magnetic line of force from the white dwarf. If the flow velocity is zero near the center of mass and reaches v_0 near r_Z, v_0 can be quite large ($\sim$2000 km s^{-1}). If the stream has uniform emissivity, at conjunctions, looking along the lines of force, emission will be shifted to $\lambda_0(1 \pm v_0/2c)$ and have full width v_0/c. At quadratures the emission is narrow and at $\lambda_0(1 \pm v_Z/2c)$, where v_Z is the rotational velocity at r_Z. Since the gravitational potential is high at r_Z, $v_0 \gg v_Z$, and the line width should vary with the apparent velocity, contrary to our contour maps (Figs. 2, 3). If the gas stream is highly curved, the emission lines may have finite width at quadratures; however, if the emissivity is highest near the white dwarf, v_0 may approach v_Z, and the velocity curves then become nonsinusoidal.

We thank J. Carrasco and G. Tuton for their help at the telescope. We are grateful to K. Shortridge and J. Fordham for their assistance in setting up and running the IPCS. J.L.G. and W.L.W.S. were supported in part by grants from the National Science Foundation AST77-09191, AST76-81089. The development of the IPCS was made possible by grants from the UK Science Research Council.

REFERENCES

Boksenberg, A., and Sargent, W. L. W. 1975, *Ap. J.*, **198**, 31.
Cowley, A. P., and Crampton, D. 1977, *Ap. J.* (*Letters*), **212**, L121.
Crampton, D., and Cowley, A. P. 1977, *Pub. A.S.P.*, **89**, 374.
Fabian, A. C., Pringle, J. E., Rees, M. J., and Whelan, J. A. J. 1977, *M.N.R.A.S.*, **179**, 9P.
Greenstein, J. L., Arp, H. C., and Shectman, S. 1977, *Pub. A.S.P.*, in press.
Hearn, D. R., and Richardson, J. A. 1977, *Ap. J.* (*Letters*), **213**, L115.
Kemic, S. B. 1974, *Wavelengths and Strengths of Hydrogen and Helium Transitions in Large Magnetic Fields*, JILA Rept., No. 113.
Krzeminski, W., and Serkowski, K. 1977, *Ap. J.* (*Letters*), **216**, L45.
Michalsky, J. J., Stokes, G. M., and Stokes, R. A. 1977, *Ap. J.* (*Letters*), **216**, L35.
Olson, E. 1977, *Ap. J.*, **215**, 166.
Priedhorsky, W. C. 1977, *Ap. J.* (*Letters*), **212**, L117.
Stockman, H. S., Schmidt, G. D., Angel, J. R. P., Liebert, J., Tapia, S., and Beaver, E. A. 1977, *Ap. J.*, **217**, 815.
Surmelian, G. L., and O'Connell, R. F. 1974*a*, *Ap. J.*, **190**, 741.
———. 1974*b*, *Ap. J.*, **193**, 705.
Szkody, P., and Brownlee, D. E. 1977, *Ap. J.* (*Letters*), **212**, L113.
Tapia, S. 1977, *Ap. J.* (*Letters*), **212**, L125.

A. Boksenberg: Department of Physics and Astronomy, University College, Gower Street, London WC1E 6 BT, England

T. A. Boroson: Steward Observatory, University of Arizona, Tucson, AZ 85721

J. L. Greenstein and W. L. W. Sargent: Department of Astronomy 105-24, California Institute of Technology, Pasadena, CA 91125